Journal of Geochemical Exploration, 32 (1989) 149–168
Elsevier Science Publishers B.V., Amsterdam — Printed in The Netherlands

The correlation between geochemical data and SPOT satellite imagery of lateritic terrain in southern Mali

C. ROQUIN, T. DANDJINOU, PH. FREYSSINET and J.C. PION

Centre de Sédimentologie et de Géochimie de la Surface (CNRS). Groupement Scientifique de Télédétection de Strasbourg. 1, rue Blessig 67084 Strasbourg Cedex, France

(Received January 21, 1988; revised and accepted September 13, 1988)

ABSTRACT

Roquin, C., Dandjinou, T., Freyssinet, Ph. and Pion, J.C., 1989. The correlation between geochemical data and SPOT satellite imagery of lateritic terrain in southern Mali. In: S.E. Jenness et al. (Editors), Geochemical Exploration 1987. *J. Geochem. Explor.*, 32: 149–168.

Detailed geochemical mapping of superficial lateritic formations is compared with recent high-resolution SPOT satellite images in the Dagadamou prospect in southern Mali.

The two main landscape features standing out in SPOT images are expressed by thematic indices derived from multispectral data. They reflect the distribution of vegetation cover and the distinction between silty clay soils in the valleys and ferruginous duricrust exposed on the plateaus. Geochemical differentiation factors are closely related to the nature of sampled materials and reflect the relative amounts of major constituent minerals estimated by normative calculation.

Duricrust samples with high Fe and Al content are also enriched in trace elements, P, V, Cr, As, Mo, Nb and Cu, immobilized in the weathering profile with secondary oxihydroxide minerals.

Soils of flats are composed mainly of quartz and kaolinite; they also concentrate heavy minerals characterized by high contents of Zr, Ti, Ce and Y.

Accumulation of detrital material at the periphery of duricrust plateaus is marked by a geochemical halo of higher contents in Zr and quartz at their periphery. This feature is clearly visible on SPOT imagery as a zone of high reflectance, devoid of vegetation.

The density of vegetation on duricrust is related to its kaolinite content. Its distribution is characterized by a striped pattern, which is probably controlled by bedrock lithological structures preserved in the lateritic cover.

This study shows the relationships, both direct and indirect, existing between spectral reflectance and geochemical composition of superficial lateritic formations. Many other landscape features identified with high resolution on SPOT images provide complementary information, which could be very helpful at various stages of geological and mineral exploration in lateritic terrain.

INTRODUCTION

In tropical areas, geological features of the bedrock are often concealed by a thick lateritic mantle and its erosion products. The combined effects of deep

0375-6742/89/$03.50

lateritic weathering and erosional processes lead to a great variety of materials exposed at the surface. It has been shown in many recent studies that efficiency of geochemical prospecting in such lateritic landscapes depends strongly on a good understanding of the nature and evolution of surficial formations. (Zeegers and Leprun, 1979; Butt, 1987).

On a Au and base metal prospect near the village of Dagadamou in southern Mali, mapping of lateritic formations is carried out with the help of recent high-resolution (20 m) SPOT satellite images. The prospect of Dagadamou covers an area of 4.5×5.5 km in the district of Kangaba, between the Mali and Guinea border and the western bank of the Niger (Fig. 1). This area was prospected in 1981 by BRGM and DNGM (Cottard et al., 1981a,b) for base metal and Au mineralization. About 1000 samples were collected in a regular 100×200 m grid, and analyzed for major and trace elements.

The main purpose of this study is to compare the multispectral and geochemical patterns of lateritic cover, with respect to geology, landscape morphology, and distribution of weathering facies. Another objective is to show the contribution of high-resolution remote-sensing data to geology and mineral exploration in tropical countries where a very thick and widespread later-

Fig. 1. Location map of studied area near the village of Dagadamou, southern Mali.

itic mantle creates major obstacles to the application of direct surface exploration methods.

DESCRIPTION OF STUDY AREA

Climate and vegetation

Southern Mali belongs to the tropical climatic zone of south Soudanian type, characterized by two contrasted seasons related to the movement of the intertropical front during the year. The mean annual rainfall is less than 1300 mm (Kamate, 1980). There is a distinct wet season between May and October. The monthly variations of temperatures range between 23° and 32°C with two maxima, corresponding to the beginning and the end of the dry season. Vegetation cover consists of a clear forested savanna with large stretches of grass and bare lands on the plateaus, where massive ferricrete is outcropping.

Geomorphology

The characteristic landforms are high plateaus of ferruginous duricrust dissected by broad flat valleys. In the western part of the Dagadamou area plateaus are higher, with monoclinal tops, and often limited by an erosion scarp. In the eastern part their shape is more rounded.

Geology

The recent geological map of Mali at 1/1,500,000 scale and its descriptive notes by Bassot et al. (1981) show that most of southern Mali is underlain by Birrimian basement rocks, formed during the Eburnean orogenesis (middle Precambrian), approximately 2000 million years ago. Several metamorphic units of ancient sedimentary and volcanosedimentary formations are separated by elongated massifs of granitic rocks (Bessoles, 1977). The study area is located at the northeastern end of the Siguiri Unit, which extends into Guinea as part of a large basin of about 40,000 km^2. The sedimentary sequence, described by Goloubinow (1950 a, b), is of flysch type. Volcanosedimentary facies (graywackes, tuffs) and volcanic or subvolcanic rocks (greenstones, rhyodacites) are also represented. They are all affected by regional metamorphism of low to intermediate grades. The stratigraphy and the distribution of the different facies are not well known, owing to the tectonic complexity and the lack of outcrop. A rather dense network of quartz veins has also been noted, sometimes related to Au mineralization.

GEOCHEMICAL SURVEY DATA

About 1000 samples were analyzed for major and trace elements by plasma emission spectrometry: SiO_2, Al_2O_3, Fe_2O_3, MgO, CaO, K_2O, MnO and TiO_2 (given in oxide percentage) and P, Ba, B, V, Cr, Co, Ni, Cu, Zn, As, Ce, Y, Sr, Zr, Li, Be, Cd, Nb, Mo, Ag, Sn, Sb, La, W, Pb and Bi (given in ppm). Au, analyzed by atomic absorption technique, showed only a few significant values. The elements for which the concentrations are generally below the detection limits (Au, Ca, Cd, Be, Ag, Sn, La, W, Pb, Bi) are not taken into account here.

Mineralogical compositions were computed from the major-element chemical analyses (Van Der Plas and Van Schuylenborgh, 1970; Grandin, 1976). Al_2O_3 was first used to calculate kaolinite [$Al_2Si_2O_5(OH)_4$]. If in excess, the remaining SiO_2 was expressed as quartz and otherwise, in the case of a deficiency of SiO_2, the excess of Al_2O_3, was expressed as gibbsite [$Al(OH)_3$].

The amount of H_2O entering in the composition of gibbsite, kaolinite and goethite [FeO(OH)] was calculated as difference between 100% and the sum of the major-element oxides. Hematite was calculated by the difference between the total Fe content and the amount of goethite.

Thus, in addition to the 34 chemical elements, one gets for each sample six

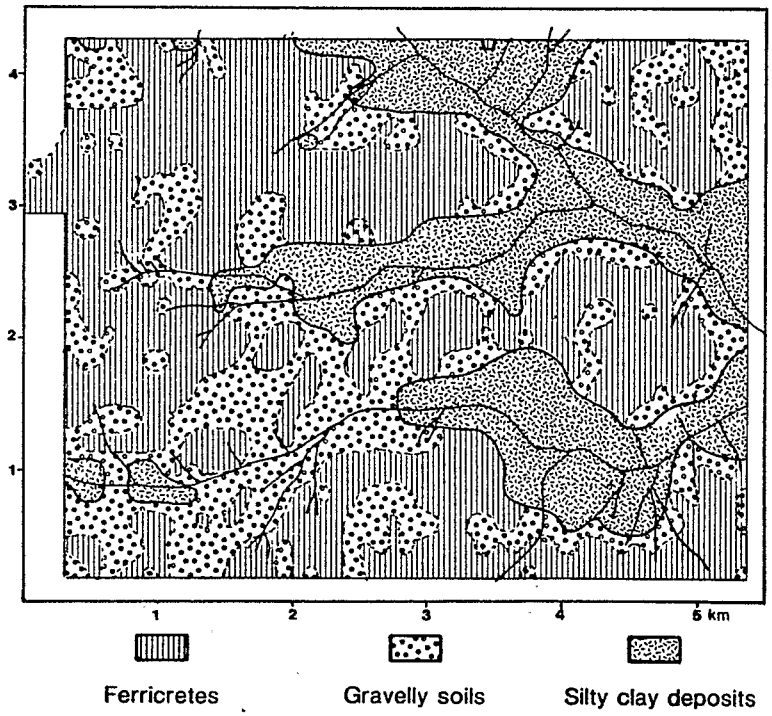

Fig. 2. Map of geochemical sampling media in the Dagadamou area, southern Mali.

mineralogical variables which are estimated contents of kaolinite (Kaol), quartz (Quar), gibbsite (Gibb), goethite (Goet, hematite (Hema) and the ratio:

$R_{HG} = 100 \times \text{hematite}/(\text{goethite} + \text{hematite})$.

Three main categories of samples have been distinguished by field observations, according to the nature of surficial materials available at each sampling site:

(a) 484 samples of massive ferruginous duricrust outcropping on plateaus.

(b) 288 samples of gravelly soils, mostly consisting of loose ferruginous nodules and duricrust fragments coming from the surficial dismantling of the ferricrete. They are often mixed in various proportion with a matrix of fine silt and clay material.

(c) 245 samples of silt and clay-rich soils overlying the duricrust in the valleys and depressions of the plateaus.

Spatial distribution of surficial formations (Fig. 2), is closely related to morphology and topography of the landscape: ferricrete facies prevail on the plateaus, while silt and clay overburden extend mainly across the flat valleys. Gravelly soils develop in intermediate positions on the slopes and at the heads of drainage networks.

GEOCHEMICAL BACKGROUND DIFFERENTIATIONS

Correlation diagrams of major elements

As can be seen on the correlation diagram between iron and silica (Fig. 3), the main trend of differentiation between samples corresponds to the opposite variations of these two elements. Aluminum is correlated with Fe (Fig. 4), but it also contributes to discriminate the three samples categories:

(a) *Soils of flats* compositions range between 70 and 85% SiO_2 and less than 10% Fe_2O_3 (Fig. 3).

(b) Within the *duricrust group* (Fig. 4), two trends of differentiation starting from the main cluster of ferruginous duricrust samples, located at 55% Fe_2O_3 and 18% Al_2O_3, can be noticed: (1) a siliceous trend corresponding to a loss of Fe and Al_2O_3 in favour of SiO_2, and (2) an aluminous trend where Al and SiO_2 are enriched in opposition to Fe.

(c) *Gravelly soils* present intermediate compositions between duricrusts and soils of flats groups. For the same level of Fe content, they show higher amounts of Al than the siliceous duricrust samples (Fig. 4).

On the correlation diagram between Al_2O_3 and Fe_2O_3 (Fig. 4), the two kinds of duricrust differentiations, aluminous and siliceous, are well separated by the mixing line between kaolinite and goethite minerals. Therefore, these two types of duricrusts have been distinguished and processed separately in this study, resulting in a total of four sampling media.

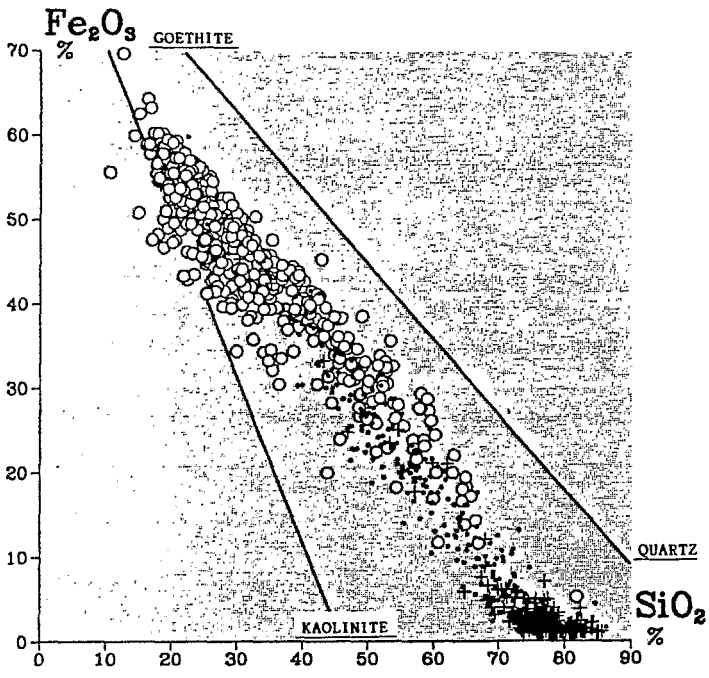

Fig. 3. Correlation diagram between SiO_2 and Fe_2O_3. + = soils of flats; ● = Gravelly soils; ○ = duricrust.

Background differentiation between sampling media

Statistical distributions of elements and minerals within the four distinct sample groups can be characterized by three parameters. The median value is used as a robust estimator of geochemical background level, while the two extreme percentiles (5% and 95%, referred to as Pct5 and Pct95 respectively) indicate its variation range. A more direct assessment of geochemical differentiation between the four facies is obtained by comparing the intra-group with the global distribution parameters. A differentiation index, D_i, was calculated as the percentage difference between intra-group and global median values relative to the global variation range of the element considered:

$$D_i = 100 \times [\text{median}(\text{group } i) - \text{median}] / (\text{Pct95} - \text{Pct5})$$

or,

$$D_i = 100 \times \text{Delta}(\text{Median}) / \text{Range}$$

This index clearly displays the geochemical contrasts between the four sampling media (Fig. 5). According to their mode of differentiation five groups of elements and minerals can be distinguished.

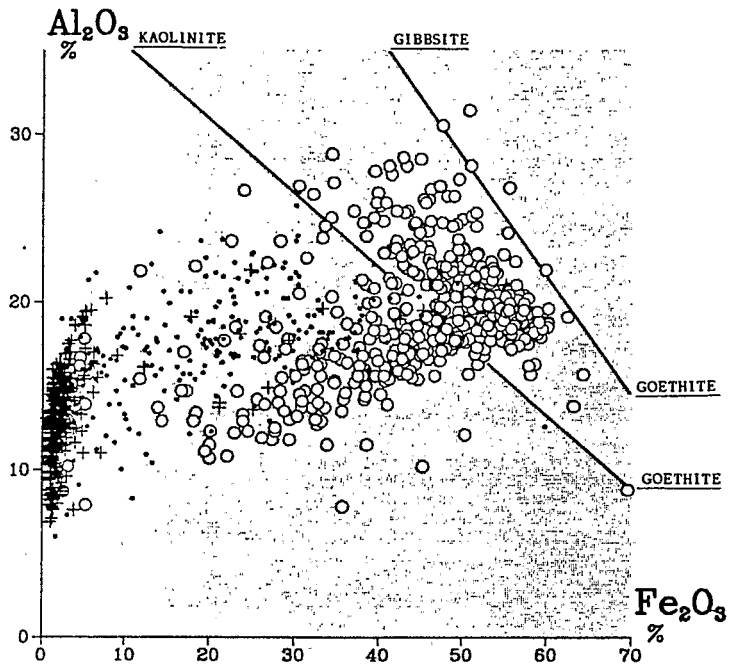

Fig. 4. Correlation diagram between Al_2O_3 and Fe_2O_3. + = soils of flats; ● = Gravelly soils; ○ = Duricrust.

(1) Elements of group I (Fe_2O_3, hematite, V, ratio (hematite/goethite), Cr, goethite, P, Mo, Nb, As) present decreasing background levels from aluminous to siliceous duricrust to gravelly soils and soils of flats.

(2) Elements of group II (Cu, Al_2O_3, kaolinite, K_2O, Ba, Ni) differ from the preceding group by higher contents in gravelly soils than in siliceous duricrust samples. MgO could also be associated with this group as its 95% percentile level is also higher in the gravelly soils. Ba and Ni show the greatest contrasts, and they are more concentrated in gravelly soils than in aluminous duricrusts.

(3) For Co (group III) the highest background is observed in siliceous duricrust. A similar trend can be noticed for the high background level of Mn, whose 95% percentile is also higher in this facies.

(4) The two mobile elements Sr and Zn, corresponding to group IV, present a rather complex behaviour. The median value of their distribution is slightly higher in gravelly and flats soils than in duricrust samples, but they display a wider range of variation with higher values in duricrust than in soils of flats samples. Such a differentiation indicates better retention of Zn and Sr in soils with an homogenization of their distribution in this environment.

(5) Elements of group V (SiO_2, TiO_2, Zr, Ce, Y) and Quartz, show a background differentiation opposite to the first group. They are accumulated in soil samples and particularly in soils of flats and depleted in duricrust samples.

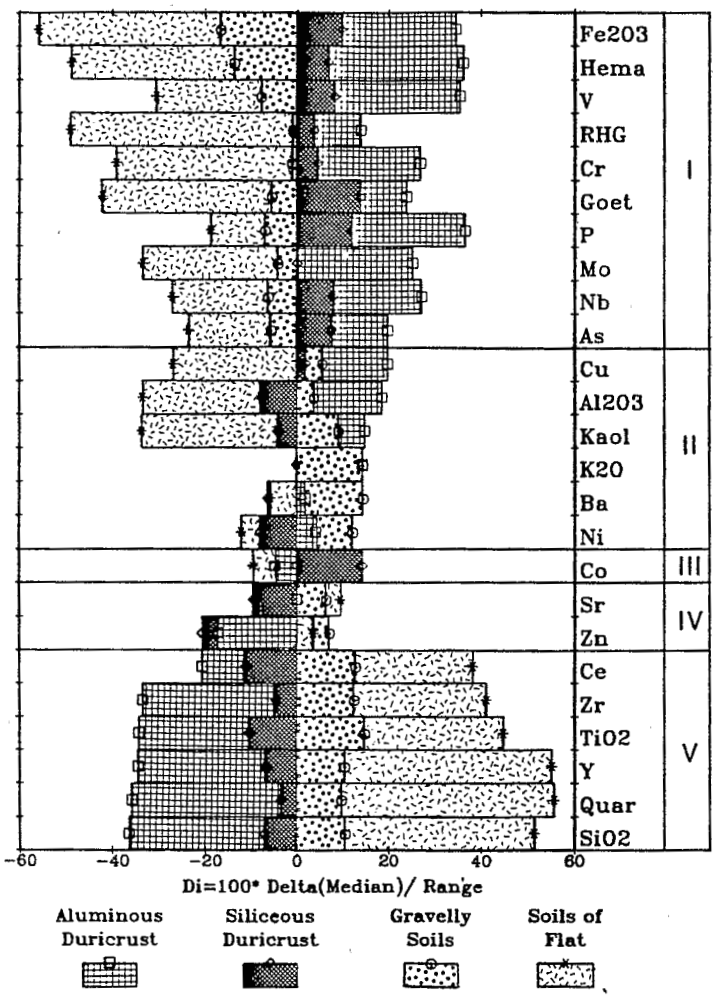

Fig. 5. Classification of elements and minerals according to their background differentation indices D_i, in the four sampling media. Goet=goethite, Hema=hematite, Kaol=kaolinite, Quar=quartz, RHG=100×Hema/(Goet+Hema).

This association is characteristic of heavy minerals (monazite, zircon, rutile, anatase, ilmenite...) accumulated with quartz in sandy covers of the valleys.

Geochemical and mineralogical associations

The main differentiation trends within each sampling facies are characterized by simultaneous variations of elements and mineral species. These geochemical and mineralogical associations can be identified on the correlation matrix (Table 1) and described by principal components analysis. This tech-

Table 1

Correlation matrix between elements and normative minerals for the whole set of background samples (N=867). Coefficient values higher than 0.4 are underlined.

	SiO2	Al2O3	Fe2O3	MgO	K2O	MnO	TiO2	Ba	P	V	Cr	Co	Ni	Cu	Zn	As	Sr	Ce	Zr	Y	Nb	Mo	Goet	Hema	Kaol	Gibb	Quar
SiO2	1.00																										
Al2O3	-.75	1.00																									
Fe2O3	-.98	.65	1.00																								
MgO	.04	.16	-.05	1.00																							
K2O	-.27	.33	.25	.29	1.00																						
MnO	-.04	-.03	.06	-.04	-.00	1.00																					
TiO2	.94	-.59	-.95	.13	-.21	-.02	1.00																				
Ba	-.10	.22	.08	.42	.48	.43	-.06	1.00																			
P	-.74	.38	.77	-.15	.16	.11	-.69	-.09	1.00																		
V	-.86	.55	.86	-.10	.11	-.01	-.84	-.01	.72	1.00																	
Cr	-.84	.64	.83	-.05	.15	-.04	-.78	.02	.61	.83	1.00																
Co	-.09	.05	.11	.13	-.08	.41	-.04	.20	.09	.07	.10	1.00															
Ni	-.24	.43	.19	.22	.18	.05	-.08	.12	.17	.06	.24	.42	1.00														
Cu	-.55	.44	.54	.01	.27	.11	-.50	.10	.42	.37	.40	.03	.35	1.00													
Zn	.13	-.01	-.15	.11	.08	.03	.20	.02	.01	-.22	-.10	-.01	.56	.31	1.00												
As	-.67	.44	.67	-.06	.18	.03	-.66	.04	.62	.67	.60	.04	.15	.41	-.03	1.00											
Sr	-.01	.20	-.03	.23	.26	.02	.02	.50	-.08	-.04	-.03	-.07	.16	.07	.20	.13	1.00										
Ce	.68	-.40	-.70	.11	-.05	.36	.71	.26	-.49	-.60	-.63	.12	-.01	-.31	.20	-.44	.23	1.00									
Zr	.95	-.72	-.93	.04	-.31	-.05	.92	-.18	-.67	-.80	-.77	-.07	-.18	-.52	.14	-.64	-.07	.62	1.00								
Y	.96	-.69	-.95	.06	-.27	.01	.95	-.07	-.67	-.81	-.81	-.05	-.15	-.50	.19	-.62	.04	.77	.93	1.00							
Nb	-.71	.39	.73	-.14	.03	-.01	-.69	-.09	.67	.92	.72	.03	.05	.29	-.18	.62	-.07	-.50	-.64	-.66	1.00						
Mo	-.74	.60	.71	-.03	.27	-.05	-.69	.03	.57	.78	.70	-.01	.22	.41	-.07	.66	.14	-.47	-.69	-.69	.79	1.00					
Goethite	-.80	.38	.81	-.07	.07	.08	-.80	-.02	.66	.72	.66	.09	.09	.42	-.12	.60	-.08	-.58	-.73	-.76	.65	.59	1.00				
Hematite	-.95	.69	.97	-.05	.30	.04	-.91	.11	.72	.83	.80	.11	.21	.53	-.14	.62	-.00	-.67	-.91	-.92	.68	.68	.63	1.00			
Kaolinite	-.65	.93	.57	.22	.37	-.03	-.50	.29	.26	.44	.52	.08	.43	.39	-.04	.35	.22	-.33	-.64	-.61	.29	.51	.34	.60	1.00		
Gibbsite	-.45	.45	.39	-.10	.01	-.01	-.38	-.11	.40	.42	.48	-.06	.13	.25	.06	.36	.00	-.30	-.41	-.38	.36	.38	.21	.43	.09	1.00	
Quartz	.99	-.82	-.96	-.01	-.30	-.03	.91	-.14	-.70	-.83	-.82	-.09	-.28	-.55	.12	-.65	-.05	.65	.94	.95	-.67	-.74	-.77	-.94	-.75	-.41	1.00
	SiO2	Al2O3	Fe2O3	MgO	K2O	MnO	TiO2	Ba	P	V	Cr	Co	Ni	Cu	Zn	As	Sr	Ce	Zr	Y	Nb	Mo	Goet	Hema	Kaol	Gibb	Quar

nique was applied with the SAS software package (1985), and the main geochemical and mineralogical patterns are represented on the first factorial plane, for each sample group (Figs. 6a–d).

On the whole a rather stable relationship is observed between mineralogical and geochemical variables. Four main associations related to the major mineral species can be identified with minor changes in the different sampling facies.

(1) A quartz and heavy-minerals association is characterized by the grouping of SiO_2 with quartz, Zr, TiO_2, Y and Ce.

(2) A ferruginous oxihydroxides association is marked by a relationship between Fe, Cr, P, V, Nb, Cu, As and Mo. Trace elements are generally better correlated with total Fe content than to either one of its normative minerals, goethite or hematite. However, Cr, Mo and Cu are preferentially linked with hematite, while P and Nb show more affinity with goethite.

(3) Aluminum, expressed mainly as kaolinite, is associated with the alkalis and alkaline earths K, Sr and Ba, and also with Ni and Cu.

(4) Manganese oxihydroxides well known properties for scavenging trace elements is expressed by correlation of MnO with Ba, Co and Ce. This coprecipitation effect appears as a rather local phenomenon but is responsible for strong anomalies in these trace elements.

Apart from those rather general patterns of differentiation, an evolution can also be observed if we compare the geochemical and mineralogical associations on the factorial diagrams of different sampling facies (Figs. 6a–d).

In *aluminous duricrust* (Fig. 6a), Ni and Co are correlated with other trace elements such as Ce, Y, Zr, and Ti, belonging to the heavy mineral phases. Trace elements associated with ferruginous oxihydroxides are better correlated with goethite than hematite, but their association with total Fe content is still higher. Gibbsite is slightly correlated with trace elements of the Fe group and more particularly with Cr.

In *siliceous duricrust* (Fig. 6b) the dominant factor corresponds to the inverse relationship between the siliceous detrital phase and the ferruginous oxihydroxide phase. Kaolinite and trace elements associated with the aluminous phase are clustered around the second factor. Nickel is well correlated with the kaolinite group, while Cu is in an intermediate position between kaolinite and hematite. On this factorial diagram, we can see that Zn and Mg are also correlated with factor 2, but their location on the negative side of factor 1 indicates a greater affinity with SiO_2 than with the Fe group. On the correlation matrix MgO is mainly associated with Ba, Sr, K_2O and Ti, whereas Zn is more correlated with Ni, Sr, Cu and TiO_2. These associations could reflect some variation in the nature of the clay mineral species present in this environment. The correlation of Ce with factor 2 shown on this diagram corresponds mainly to an association with Ba, due to their simultaneous enrichment in manganese hydroxides.

For *gravelly soils* (Fig. 6c), the geochemical pattern presented on the first

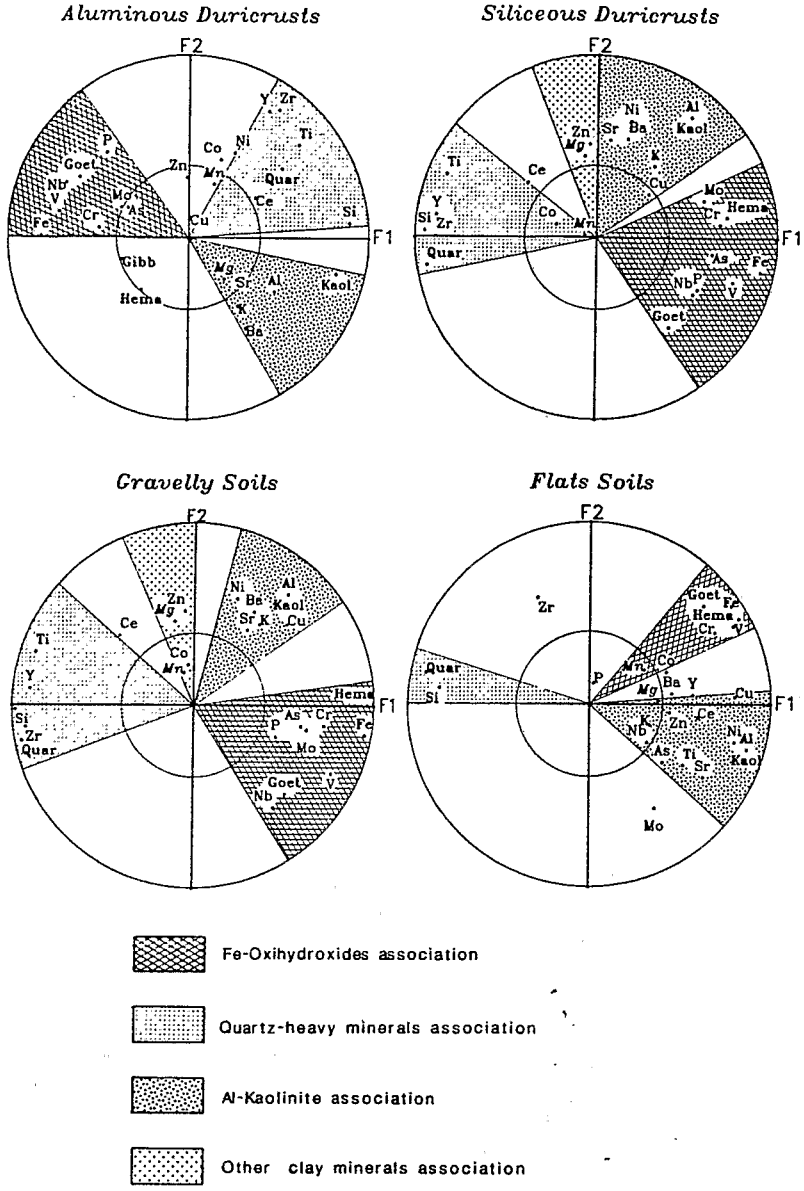

Fig. 6. Representation of elements and minerals in the first factorial plane of principal components analysis within each sampling media: (a) aluminous duricrust; (b) siliceous duricrust; (c) gravelly soils; (d) soils of flats.

factorial plane is fairly similar to that described previously for siliceous duricrust. There is, however, a better distinction between the different associations.

In *soils of flats* factorial diagram (Fig. 6d) we observe, on the contrary, many

important changes between mineral and trace-element associations. Quartz, as the dominant phase, is opposed by a strong dilution effect to all the other elements except Zr, which keeps a slight positive correlation ($r=0.35$) with this mineral. Most of the trace elements are clustered around the kaolinite association, which is more abundant in this facies than Fe oxihydroxides. Such a trend is particularly noticeable for Ti and Ce, no more associated with quartz and silica. In this sample group, only Cr and V are preferentially associated with iron oxihydroxides rather than with the kaolinite association.

GEOCHEMICAL MAPPING

Geochemical maps of Fe (Fig. 7), kaolinite (Fig. 8) and Zr (Fig. 9) illustrate the main differentiation trends of element distributions in this area and allow another view of the geochemical patterns already described with the statistical methods. They are drawn with the use of the UNIRAS (1984) graphic software library. Variations of element contents are represented on a grey scale, after linear interpolation between sampling points.

A sharp contrast is observed between values for outcropping ferricrete on the plateaus and those from silty clay covers in the valleys. Extension of plateaus is delineated by high background levels in Fe_2O_3, Al_2O_3, Cr, V, P, Cu, As, Mo, Nb, goethite, hematite and kaolinite. On the contrary, flats are enriched

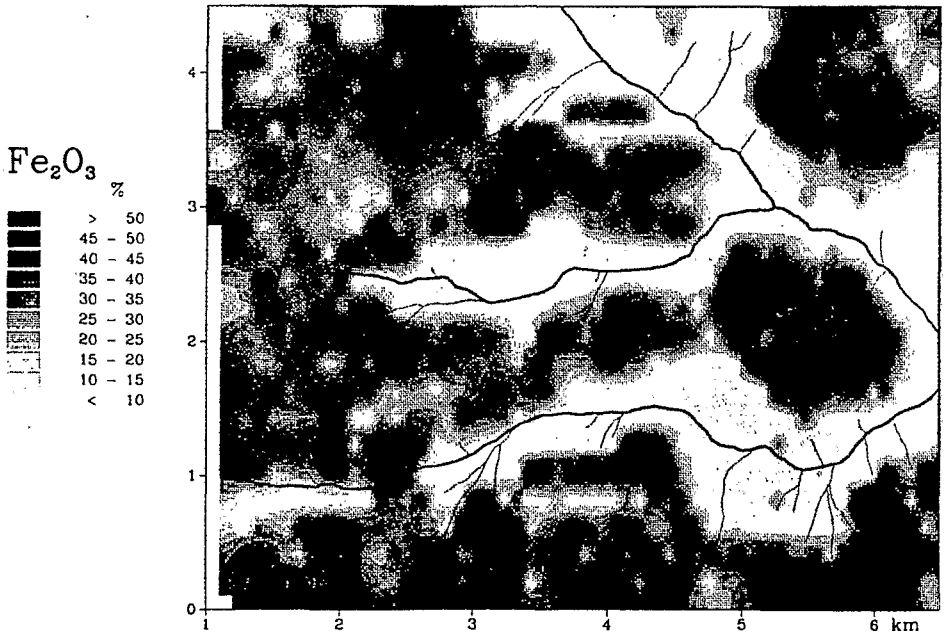

Fig. 7. Geochemical map of Fe.

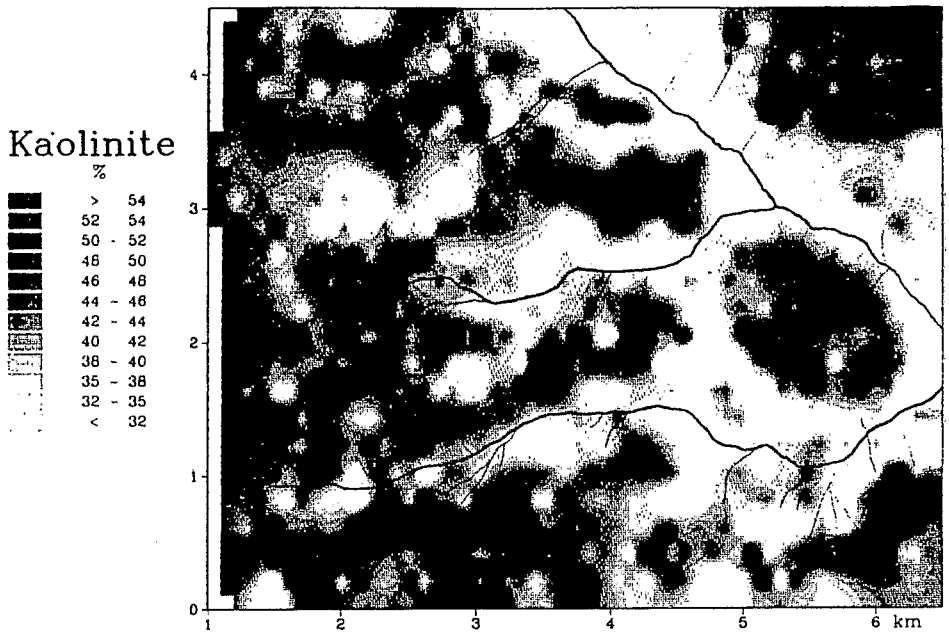

Fig. 8. Geochemical map of normative kaolinite, calculated from geochemical data.

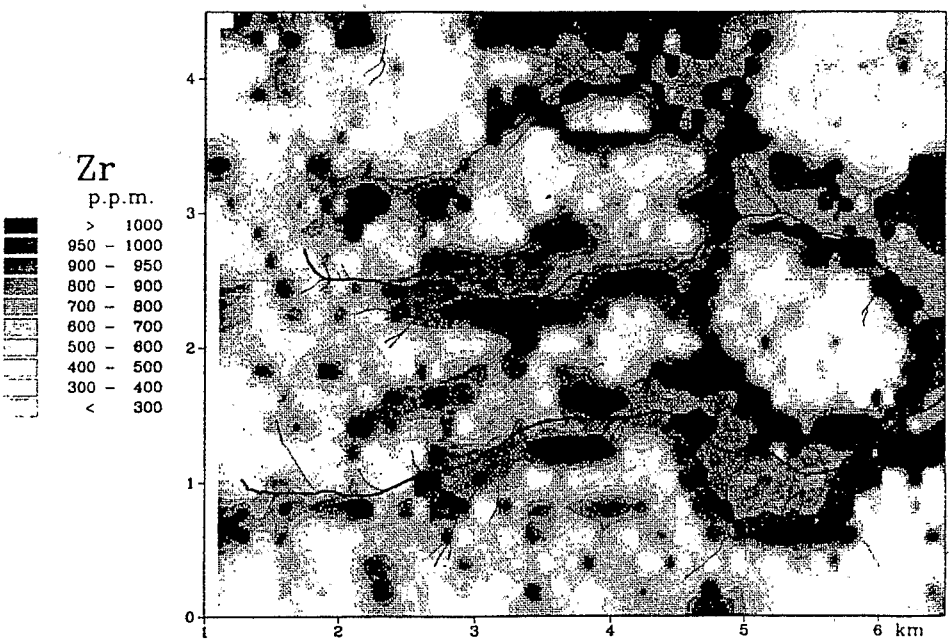

Fig. 9. Geochemical map of Zr.

in quartz, SiO_2, TiO_2, Zr, Ce and Y. There is no evidence of another kind of regional differentiation related to lithological variations of underlying bedrock; although some high-value patterns in As, Cr, V and Sr suggest a structural control stretching in the NNW–SSE direction.

Another, more conspicuous, pattern corresponds to a halo of high concentrations in Zr (Fig. 9) and, less extensively, in quartz content, outlining ferricrete plateaus. This feature is particularly noticeable in the eastern part of the area around an isolated butte of duricrust, near the village of Dagadamou. It could be related to a pedological differentiation corresponding to the bottom slope detrital accumulation of zircon and quartz minerals at the periphery of plateaus, with further leaching of fine clay particles. Absence of such zoning pattern for Ti, Ce, and Y, which are also enriched in soils of flats, confirms the distinct behaviour of these elements, noted previously on the factorial correlation diagram in this environment (Fig. 6d).

SPOT IMAGES

SPOT satellite remote sensing data of this area (scene 39-326) have been acquired at the end of the dry season on 5 April 1986 at 11 a.m. It is an oblique view with 25° incidence, in the multispectral mode of the HRV radiometer (Begni, 1982; Baudoin, 1982). Measures of reflectance are given in three spectral bands corresponding to XS1 (0.50–0.59 μm) and XS2 (0.61–0.68 μm) in the visible range and to XS3 (0.79–0.89 μm) in the near infrared domain. After standard geometric rectification (level 1B) the pixel size of the image is of 20 x 20 m.

After rotation and registration of SPOT image with geochemical maps, using roads and drainage network as reference landmarks, a window of 225 x 275 pixels, corresponding to the survey area was selected.

The main geomorphological units of the landscape are easily identified by variation of reflectance in the three spectral bands XS1, XS2 and XS3.

Duricrust materials exposed at the surface of plateaus have lower albedo than the silty clay soils of the valleys and appear in darker grey levels on images of XS1 and XS2. A better discrimination is obtained by taking into account the difference of colors between superficial formations, perceived as a slight contrast between the two visible bands XS1 and XS2. A synthetic index, reflecting both albedo and color contrasts (Roquin et al., 1987) is expressed as:

$$Ic = 3 \times XS1 - XS2 - 100$$

An image of this index (Fig. 10) clearly reflects the main differentiation pattern already observed on geochemical maps (Fig. 7, 8, 9). Limits of plateaus are delineated in greater detail due to the higher resolution of SPOT images. The drainage network in the valleys is also well marked by low intensities corresponding to the development of gallery forest along the stream channels.

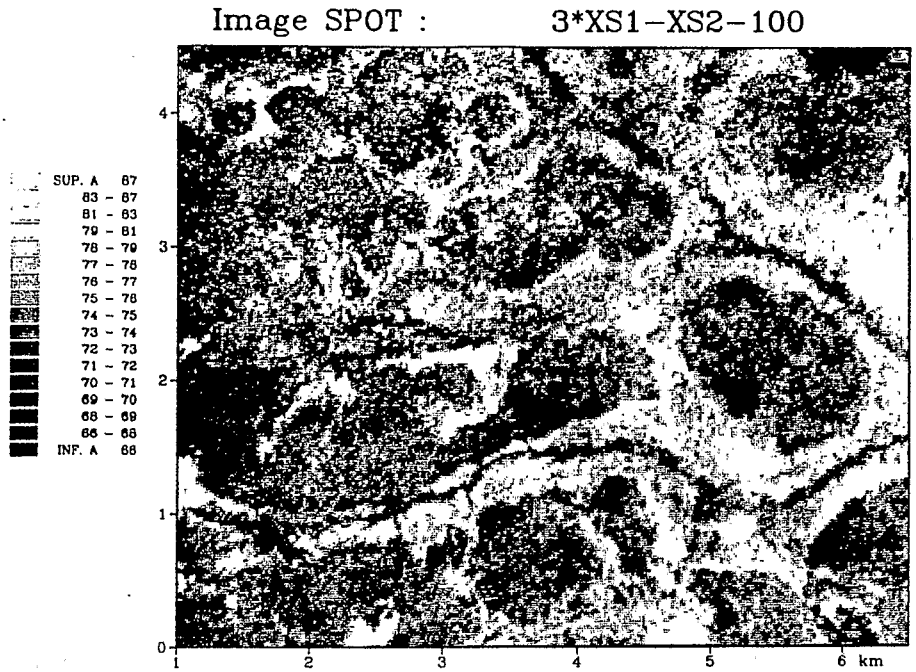

Fig. 10. SPOT image of the duricrust index: $Ic = 3 \times XS1 - XS2 - 100$.

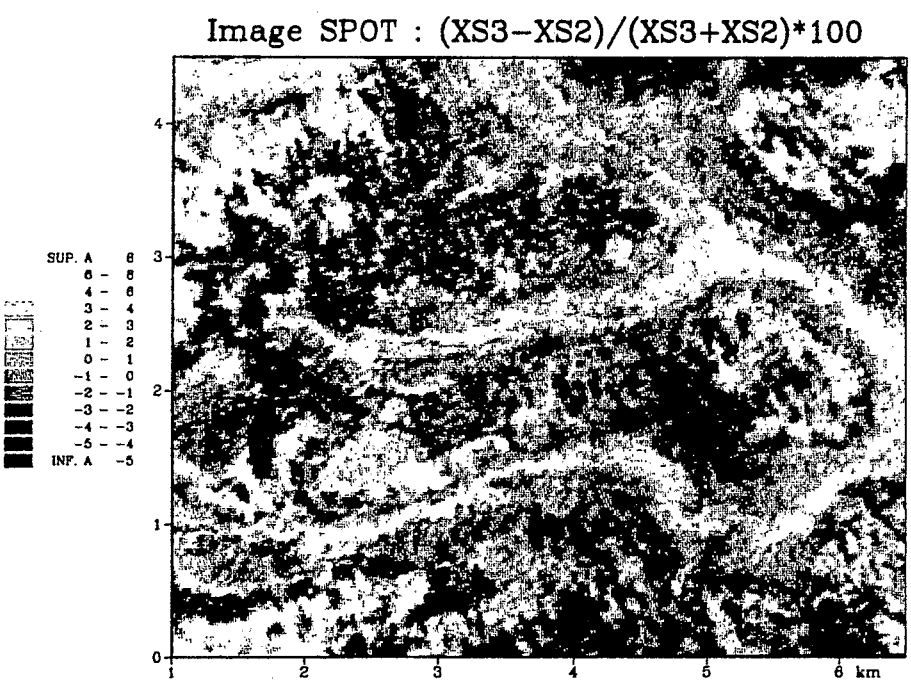

Fig. 11. SPOT image of the vegetation index: $Iv = 100 \times (XS3 - XS2)/(XS3 + XS2)$.

A narrow strip of high reflectivity outlines the margins of plateaus. It corresponds to the geochemical halo observed for Zr and Silica on geochemical maps.

Influence of vegetation, still important at this season, is characterized by high intensities in infrared band XS3 and relatively low intensities in the visible bands XS1 and XS2. This spectral signature is expressed by the vegetation index, Iv, (Cliche et al., 1982; Saint and Podaire, 1982) represented on Fig. 11..

$$Iv = 100 \times (XS3 - XS2)/(XS3 + XS2)$$

We can see on Fig. 11, that vegetation is more developed in the valleys and along the stream courses.

On several plateaus, alternate bands of vegetation and bare duricrust outcrops form a striped pattern, stretching in the NW–SE direction. This distribution feature of the vegetation cover is probably an expression of lithological structures preserved in the lateritic cover and may be considered as good evidence of the residual character of the weathering profile. Similar features have already been observed by Mainguet (1978) in the Central African Republic.

GEOCHEMICAL AND REMOTE SENSING DATA CORRELATIONS

In order to see more precisely how the spectral signature of lateritic covers on SPOT image could reflect their geochemical and mineralogical composition, correlations between the two data sets were also studied. Every pixel corresponding to a sampling site was first sampled on the SPOT image and then the radiometric and geochemical data files were merged.

Correlations with duricrust and vegetation indices, which provide a good summary of multispectral information, are considered here. Highest correlation coefficients values (>0.1) of elements or normative minerals with each index have been plotted on diagrams given for the whole sample set (Fig. 12) and separately for each sampling facies (Fig. 13a–d).

On the diagram of correlation coefficients for the whole sample set (Fig. 12) elements are clustered in three main groups, according to their geochemical background differentiation pattern:

(1) Quartz and silica, with their associated trace elements Ti, Y, Zr and Ce, are positively correlated with the vegetation and duricrust indices;

(2) In contrast, the Fe group with goethite, V, P, Nb, As, Mo and Cr show negative correlations with the two indices;

(3) The kaolinite of Al group encompass a wider range of intermediate values. At one end there is a more strongly negative correlation of the duricrust index with the less mobile elements (Al, kaolinite, Cu), enriched in the ferricrete. At the other end a positive correlation with the vegetation index is observed for

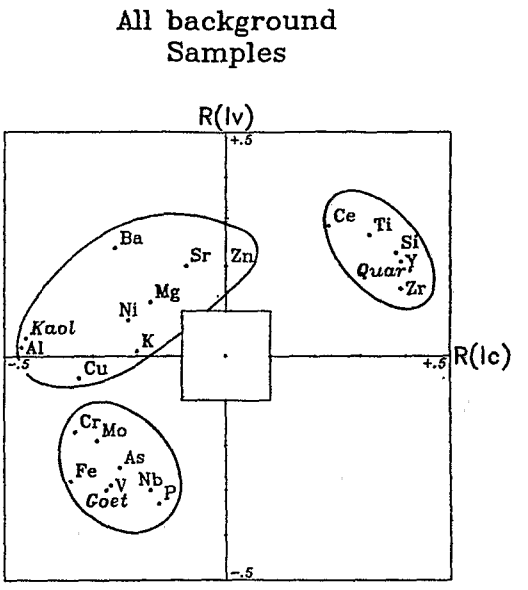

Fig. 12. Diagram of elements and normative minerals correlation coefficients with duricrust index, R(Ic), and vegetation index, R(Iv), for all background samples.

the more mobile elements (Ba, Sr, Zn, Mg, Ni), preferentially concentrated in gravelly soils or soils of flats.

Several modifications of these relationships are observed when they are considered separately, within each facies (Fig. 13a–d).

In the three duricrust facies (aluminous, siliceous or gravelly), a common feature corresponds to the positive correlation of Al and kaolinite and some associated trace elements with the vegetation index. Such an affinity between vegetation and kaolinite content of duricrust was already noticed in western Africa by Maignien (1958). The opposite behaviour is observed for quartz, silica and associated trace elements, which are positively correlated to the duricrust index and inversely correlated to the vegetation index.

In every case, the response of Fe is not predominant and is evolving from one facies to another. In aluminous duricrust it is similar to quartz and silica, whereas in gravelly soils it shows the same kind of signature as kaolinite and Al. It can be noticed however, that phosphorus tends to stay negatively correlated with the vegetation index in the three duricrust facies.

In soils of flats, geochemical composition is reflected in a different way by the two radiometric indices.

Barium, Ce, Mn, Sr and Co are positively correlated with the vegetation index and negatively correlated with the duricrust index. This suggests that manganese concretions develop mainly in environments favorable for vegeta-

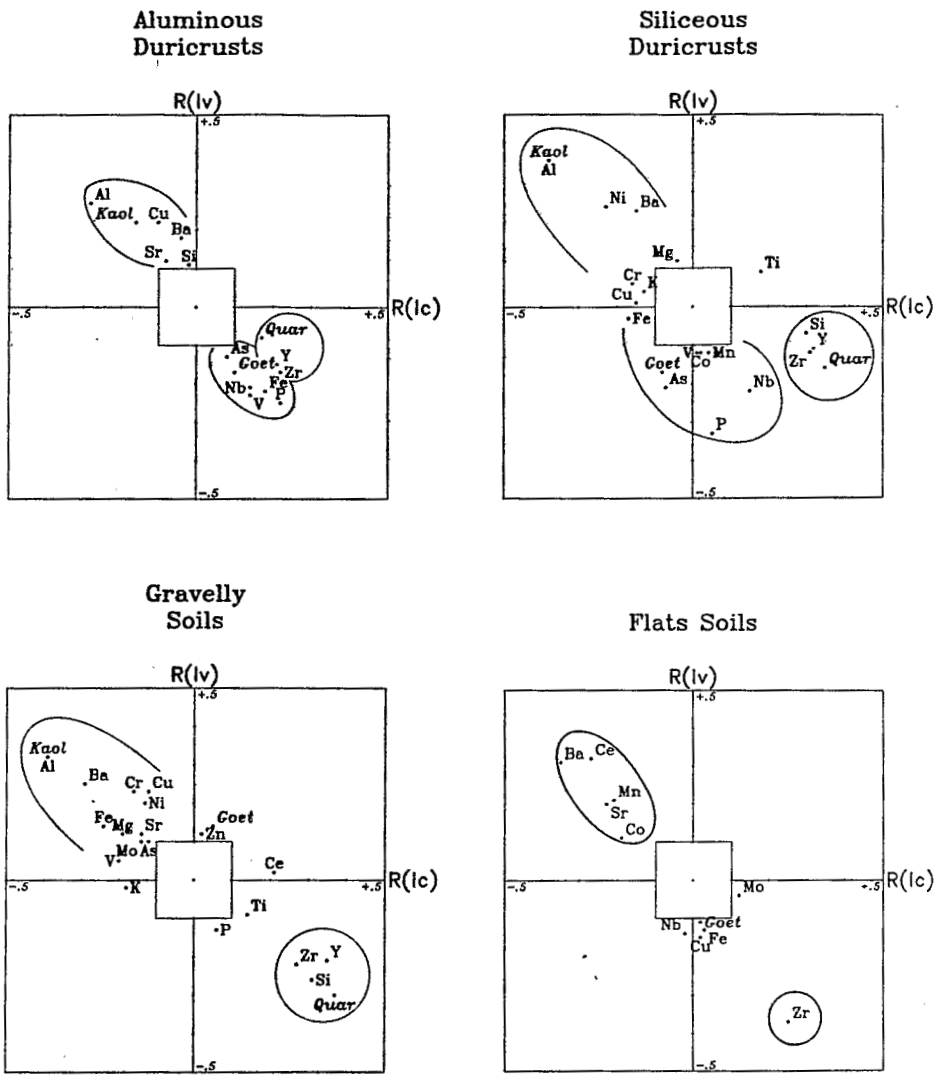

Fig. 13. Diagram of elements and normative minerals correlation coefficients with duricrust index. R(Ic), and vegetation index, R(Iv), within each class of sampling media: (a) aluminous duricrust; (b) siliceous duricrust; (c) gravelly soils; (d) soils of flats.

tion, either at the emergence of the water table or along the stream channels, where some humidity is kept longer during the dry season.

On the contrary, Zr in soils of flats is correlated with the duricrust index and opposed to the vegetation index. This simply reflects the correspondence between the geochemical halo of Zr outlining the plateaus, and the halo of high reflectance without vegetation observed on SPOT images.

CONCLUSIONS

This study brings out many examples of relationships existing between multispectral and geochemical signatures of lateritic covers in the south of Mali.

The differentiation of superficial formations, dominated by the contrast between ferruginous duricrust on the plateaus and silty clay soils in the valleys, is an image of the geomorphological evolution of the landscape. Two different features of this evolution are clearly illustrated on both SPOT images and geochemical maps.

(a) The residual character of the lateritic weathering profile is pointed out by the striped pattern of vegetation distribution on duricrust plateaus, reflecting some control by bedrock lithology. The density of vegetation is also related to the abundance of kaolinite in the duricrust.

(b) On the contrary, mechanical dispersion of detrital materials, accumulated in the valleys is evidenced by a halo of quartz and zirconium at the bottom slope of duricrust plateaus. Another way of mobilization exists for elements like Ti, Ce and Y, which are also accumulated in thalweg soils, but do not display the same zoning pattern. They seem to be further transported downwards, with the leaching of fine clay particles.

The difference of chemical mobility between elements is also reflected by their distribution in the landscape:

(a) Less mobile elements (P, V, Cr, As, Mo, Nb, Cu), following Fe oxyhydroxides, accumulate in duricrust exposed on the plateaus.

(b) Kaolinite is also more abundant in duricrust, but its associated trace elements (K, Ba, Ni, Sr, Mg, Zn) are relatively enriched downslope in gravelly soils and soils of flats.

(c) Manganese oxyhydroxides with high concentrations in Ba, Co and Ce, are better retained in siliceous duricrust than in the other facies.

Multispectral information provided by SPOT images is very useful to identify many physiographic features of the landscape and the differentiation of superficial formations of the lateritic cover. It can contribute to the elaboration of a model of landscape evolution, and the definition of a prospecting strategy adapted to each kind of environment.

ACKNOWLEDGEMENTS

We are very grateful for the support given to this study by Centre National d'Etudes Spatiales (CNES) for SPOT remote sensing data, and to Bureau de Recherches Géologiques et Minières (BRGM) and Direction Nationale de la Géologie et des Mines (Mali) (DNGM) for their help and communication of the results of geochemical prospection.

REFERENCES

Bassot, J.P., Meloux, J. and Traoré, H., 1981. Notice explicative de la carte géologique à 1/1,500,000 de la Republique du Mali. DNGM-BRGM, 137 pp.

Baudoin, A., 1982. Les applications cartographiques de SPOT à l'Institut Géographique National-France. Bull. IGN, 44:38-49.

Begni, G., 1982. La qualité des images SPOT. Colloque de Montréal, 1982. In: Le système SPOT d'observation de la Terre. Assoc. Que. Télédetection/Soc. Fr. Photogramm. Télédetection, pp. 33-46.

Bessoles, B., 1977. Geologie de l'Afrique. Le craton ouest africain. Mem. BRGM, 88, 402 pp.

Butt, CRM, 1987. A basis for geochemical exploration models for tropical terrains. Chem. Geol., 60: 5-16.

Cliche, G., Bonn, F., Dupont, O., Carignan, M. and Charbonneau, L., 1982. Une étude comparative de simulations SPOT et Landsat-D dans un milieu agricole et periurbain du sud du Québec. Colloque de Montréal, 1982. In: Le système SPOT d'observation de la Terre. Assoc. Que. Télédetection/Soc. Fr. Photogramm. Télédetection, pp. 111-124.

Cottard, P., Dommanget, A., Keita, M., and Zeegers, H., 1981a. Prospection d'or, district de Kangaba. Campagne 1979-1980. Rap. BRGM., ref.81 RDM 003 AF (unpubl.).

Cottard, P., Dommanget, A., and Keita, M., 1981b, Prospection aurifère sur le permis Kéniéba-Kangaba. Campagne 1980-1981. Rapp. BRGM, ref.81 RDM 058 AF (unpubl.).

Goloubinow, R., 1950a. Notice explicative sur la feuille de Kankan Est. Carte de reconnaissance à 1/500,000. Gouv. Gen. AOF, Dakar, 28 pp.

Goloubinow, R., 1950b. Notice explicative sur la feuille de Bougouni Ouest. Carte de reconnaissance à 1/500,000 Gouv. Gen. AOF, Dakar, 23 pp.

Grandin, G., 1976. Aplanissements cuirassés et enrichissement des gisements de manganèse. Mèm. ORSTOM, Paris, 268 pp.

Kamate, C., 1980. Climat. In: Atlas du Mali. Les Atlas jeune Afrique, les éditions j.a., Paris, 1980, 64 pp.

Maignien, R., 1958. Le cuirassement des sols en Guinée. Mém. Serv. Carte Géol. Alsace Lorraine, 18, 239 pp.

Mainguet, M., 1978. Quelques aspects de la détection et de l'insertion spatiale des phénomènes de cuirassement sur les photographies aériennes et images satellites. In Géomorphologie des reliefs cuirassés dans les pays tropicaux chauds et humides. Trav. Doc. Géogr. Trop., CEGET, 33: 209-229.

Roquin, C., Dandjinou, T., Freyssinet, Ph., Pion, J.C. and Tardy, Y., 1987. Premiers résultats de cartographie des couvertures latéritiques par images Spot, région de Kangaba (Sud-Mali). C.R. Acad. Sci. Paris, vol. 304, Sér. II, 8: 321-326.

Saint, G. and Podaire, A., 1982. Comparaison des capteurs de Landsat-D et de SPOT sur le thème agriculture. Colloque de Montréal, 1982. In: Le système SPOT d'observation de la Terre. AQT/SFPT: 193-204.

SAS, 1985. User's Guide: Statistics, Version 5 Edition. SAS Institute Inc., Cary, NC, U.S.A., 956 pp.

UNIRAS, 1984. GEOPAK User's Manual, Version 84:2. European Software Contractors A/S, Lyngby, Denmark,: 325 pp.

Van Der Plas, L. and Van Schuylenborgh, H, 1970. Petrochemical calculations applied to soils with special reference to soil formation. Geoderma, 4: 357-385.

Zeegers, H. and Leprun, J.C., 1979. Evolution des concepts en altérologie tropicale et conséquences potentielles pour la prospection géochimique en Afrique occidentale soudano-sahélienne. Bull. BRGM, II, 2-3: 229-239.